Neutron beam optimization based on a ^{7}Li(p,n)^{7}Be reaction for treatment of deep-seated brain tumors by BNCT

Zahra Ahmadi Ganjeh S. Farhad Masoudi[1)]

Department of Physics, K. N. Toosi University of Technology, P. O. Box 15875-4416, Tehran, Iran

Abstract: Neutron beam optimization for accelerator-based Boron Neutron Capture Therapy (BNCT) is investigated using a ^{7}Li(p,n)^{7}Be reaction. Design and optimization have been carried out for the target, cooling system, moderator, filter, reflector, and collimator to achieve a high flux of epithermal neutron and satisfy the IAEA criteria. Also, the performance of the designed beam in tissue is assessed by using a simulated Snyder head phantom. The results show that the optimization of the collimator and reflector is critical to finding the best neutron beam based on the ^{7}Li(p,n)^{7}Be reaction. Our designed beam has 2.49×10^{9}n/cm^{2}s epithermal neutron flux and is suitable for BNCT of deep-seated brain tumors.

Key words: BNCT, target design, ^{7}Li(p,n)^{7}Be reaction, beam shaping assembly, dosimetry

PACS: 87.53.Bn, 28.20.Gd, 29.25.Dz **DOI:** 10.1088/1674-1137/38/10/108203

1 Introduction

It is difficult to treat the deep seated brain tumors via surgery or other conventional therapies. Boron Neutron Capture Therapy (BNCT) is an effective therapeutic modality for these tumors. This method benefits the thermal neutron capturing by ^{10}B, due to its large absorption cross section for a thermal neutron, and the breaking of ^{11}B excited nucleus into an alpha particle and a ^{7}Li ion. These particles deposit their energy over distances less than 10 μm - which is comparable to the cell diameter - and destroy tumor cells with negligible damage to the healthy tissue [1–3]. The success in this method depends on the injection of the ^{10}B carrier drug and irradiation of the tumor area by suitable neutron beam. The most suitable neutron energies for treating deep-seated tumors are 1 eV–10 keV which are named the epithermal energy range. Epithermal neutrons slow down to the thermal energies via passing through different tissues before reaching the tumor [3, 4].

Nuclear reactors are practical neutron sources for BNCT, however, they have some disadvantages such as their high cost and low social acceptability and problems related to their installation and operation in hospitals. To dominate such problems, using accelerator-based neutron sources has been proposed. The advantages of using these sources are: simple application, high safety in hospital environments, relative low cost compared with reactors, easy turning off, providing sufficient neutron flux, and less overall risk than nuclear reactors. However, the most crucial aspects for accelerator-based neutron sources are the type and energies of incident particles, and target material selection [5–8].

The most common reaction for BNCT is ^{7}Li(p,n)^{7}Be with a 1.644 MeV Q-value, and 1.881 MeV proton threshold energy. This source produces a high flux neutron with a relatively low energy. In spite of these advantages, its serious drawback is its low melting point (180 ℃) of lithium and its low thermal conductivity (84.7 W/m°k). In this article, we design a suitable configuration based on a ^{7}Li(p,n)^{7}Be reaction by using the MCNP-X code to have a proper neutron beam which satisfies the IAEA criteria for BNCT. Our desigh contains a cooling system, moderator, reflector and collimator. It has been shown that the optimization of the reflector and collimator is critical to have a high epithermal flux. Also, by dosimetric calculation in a simulated head phantom, we have shown that the designed neutron beam is suitable for treating deep-seated brain tumors by BNCT.

Table 1 shows the IAEA critria where $\Phi_{\rm epi}$ and $\Phi_{\rm th}$ are the fluxes of epithermal and thermal neutrons, and $\dot{D}_{\rm f}$ and $\dot{D}_{\gamma}$ are the dose rates of fast neutrons and gamma.

Table 1. IAEA recommended in-air parameters for BNCT [9].

BNCT beam port parameters	limits
$\Phi_{\rm epi}$/(n/cm^{2}s)	$>0.5\times10^{9}$
$\Phi_{\rm epi}/\Phi_{\rm th}$	>20
$\dot{D}_{\rm f}/\Phi_{\rm epi}$/(Gy cm^{2})	$<2\times10^{-13}$
$\dot{D}_{\gamma}/\Phi_{\rm epi}$/(Gy cm^{2})	$<2\times10^{-13}$

Received 4 November 2013

1) E-mail: masoudi@kntu.ac.ir

2 Materials and methods

2.1 Target and cooling system

While the ^{7}Li(p,n)^{7}Be reaction is suitable as accelerator-based neutron sources for BNCT, there are several drawbacks related to the mechanical, chemical, and thermal properties of metalic lithium [10, 11].

Replacing lithium with beryllium and carbon targets has been suggested by many researchers in order to overcome these problems. While the melting point and thermal conductivity of Beryllium and Carbon targets are higher than metallic lithium, the lithium target produces a higher neutron flux with an average energy less than two others [12]. So, in our designing, we used metallic lithium as a target to be bombarded by the proton beam.

A cooling system was designed to reduce the volumetric heat deposited on the target [12]. In recent years, a rib structure for the coolant path has been proposed by researchers for more efficient heat removal [13]. Following this work, a rib structure was used for the coolant path in the backing plate of the target. The materials of the cooling system are chosen in a way that they moderate the fast neutrons and increase the epithermal neutron flux at the end of the cooling system. In all simulations, the backing plates contain thirteen 15 mm×10 mm rectangular channels. As the effects of fluid flow on neutron flux can be ignored, we simulate the stagnant cooling liquid inside the channels in the MCNP code in which the fluid liquid can not be simulated.

2.2 Target temperature

Considering the proposed cooling system, we calculate the temperature of the lithium layer by $T_{\rm Li} = \Delta T_{\rm Li}+\Delta T_{\rm b}+\Delta T_{\rm b-h}+\Delta T_{\rm h}+T_0$ [11] where $\Delta T_{\rm Li}$, $\Delta T_{\rm b}$, $\Delta T_{\rm b-h}$ and $\Delta T_{\rm h}$ are the drop temperatures of the lithium layer, backing plate, backing surface-heat carrier, and heat carrier (cooling liquid), respectively. Also T_0 is the initial temperature of the heat carrier.

The drop temperature for lithium is estimated by $\Delta T_{\rm Li}=(0.5)(q_{\rm Li})(h_{\rm Li})/\lambda_{\rm Li}$ where $h_{\rm Li}$ is the lithium thickness, $\lambda_{\rm Li}$ is the heat conductivity, and coefficient 0.5 denotes the deposited volumetric heat on the target. Also, $q_{\rm Li} = qh_{\rm Li}/L$ is the power density released in lithium where L is the path of protons in the lithium target. Also the drop temperature for backing is $\Delta T_{\rm b}=q_{\rm b}h_{\rm b}/\lambda_{\rm b}$, where $h_{\rm b}$ and $\lambda_{\rm b}$ are the thickness and heat conductivity of the backing plate.

Drop temperature of the backing plate-heat carrier is $\Delta T_{\rm b-h} = q/\alpha$ [14]. Here α stands for the heat transfer coefficient from the backing to heat carrier which is $\alpha = (Nu)(\lambda)/d$, where λ is the heat conductivity of the heat carrier and d is the equivalent diameter of the flow path ($d = 4S/P$, where S is the cross sectional area of the channel, and P is its circumference). Also Nu is the Nusselt number which is determined by $Nu = (0.023)(Re)^{0.8}(Pr)^{0.4}$ where Re and Pr are the Reynolds and Prandtl numbers. These numbers depend on the coolant speed (v), kinematic viscosity (ν), specific heat ($C_{\rm p}$) and density of the heat carrier (ρ) as $Re=(v)(d)/\nu$ and $Pr=(C_{\rm p})(\nu)(\rho)/\lambda$.

2.3 BSA optimization

In order to make an available neutron beam for BNCT of deep-seated brain tumors, a well-defined epithermal neutron spectrum is required. We design and optimize a beam shaping assembly (BSA) for the neutrons at the end of the cooling system. The method is based on finding the optimum materials and geometries in a way that the beam contamination is removed as much as possible and the IAEA recommended criteria (see Table 1) are satisfied. Different parts are designed in BSA as follows.

Moderator: We examine the most suitable materials as moderator in order to slow down the fast neutrons close to the desired epithermal range without broadening the neutron spectrum simultaneously.

Reflector: A reflector is used in order to avoid exiting neutrons before reaching the beam port and stabilizing neutrons economy. We examine materials with a low absorption cross section and high elastic scattering cross section for epithermal energies, while having a large mass number in order to the lessen energy loss with each elastic collision [15].

Thermal neutron filter: Since the thermal neutrons are captured more efficiently by ^{10}B, which occurs in both the tumor and normal cells, the presence of these neutrons in the beam damages the shallow tissues before reaching the tumor. Therefore, it is essential to utilize some materials to remove these low energy neutrons before leaving the BSA. We investigate proper materials as thermal neutron filters, and their quality is assessed by the in-air parameters.

Collimator: In order to guide neutrons to the patient position and to have a local radiation to the brain, the diameter of irradiated beam should be reduced to 12–14 cm [9]. In the proposed configuration, the BSA beam port is decreased to a 6 cm-radius flat circular surface by using a proper collimator.

2.4 Methodology of dose evaluation

To evaluate the dosimetric performance of the designed beam, the in-phantom parameters are benefited. While the in-air parameters are tallied at the BSA beam port, the in-phantom parameters are calculated in a simulated head phantom to reflect the therapeutic effects of the irradiated beam. These parameters include[4]: Advantage Depth (AD), which indicates the depth of effective penetration over which a therapeutic gain is realized;

AD Dose Rate (ADDR), which is the maximum delivered dose rate to the healthy tissue; Treatment Time (TT), that can be estimated considering the maximum tolerable dose to the healthy tissue (12.5 Gy); and Advantage Ratio (AR) which is the ratio of the total therapeutic dose in the tumor to the total normal tissue dose over a given depth (usually from the surface to AD).

We simulated the Snyder head phantom which consists of skin, a skull and a brain with a centrally located tumor for calculation of the total physical dose ($D_{\rm T}$). $D_{\rm T}$ is the sum of physical dose components multiplied by weighting factors (denoted by ω) of each component ($D_{\rm T}=\omega_{\rm N}\cdot D_{\rm N}+\omega_{\gamma}\cdot D_{\gamma}+\omega_{\rm fast}\cdot D_{\rm fast}+CBE\cdot D_{\rm B}$) where $D_{\rm N}$, D_{γ}, $D_{\rm fast}$, and $D_{\rm B}$ stand for thermal neutron, gamma, fast neutron and boron dose, respectively, and CBE is the compound biological effectiveness.

3 Result and disscusions

3.1 Target

We considered lithium with cylindrical geometry with 10 μm in thickness. The simulation results show that the number of produced neutrons does not increase by increasing the lithium thickness of more than 100 μm. Also, lithium is better than other lithium compounds like LiF, Li_2O, LiH and Li_3N, because the neutron production with lithium is at least 40 percent more than others. Fig. 1 shows the neutron spectrum corresponding to the 100 μm thick lithium target bombarded by a 2.5 MeV–20 mA proton beam. By the result, the produced neutrons are approximately fast, and so they must be slowed down to epithermal neutrons to be proper for BNCT of deep-seated brain tumors.

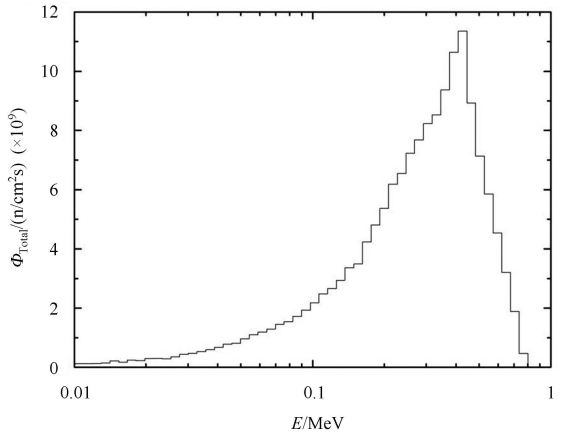

Fig. 1. (color online) Neutron spectrum corresponding to the 100 μm thick lithium target.

3.2 Cooling system

In order to choose the best material as the backing plate, we investigated the effect of 5 different materials with a high heat conductivity on neutron production. Table 2 presents the simulation results for these materials, where H_2O has been used as the cooling liquid. As the calculated epithermal neutron flux and the total number of neutrons (N) corresponding to Al were more than others, it was selected as the backing plate for the lithium target. Moreover Al is an interesting metal due to its fairly low cost.

In order to select a suitable cooling liquid for heat transfer, H_2O, Hg (liquid), and Ga(liquid) were proposed. Table 3 presents the comparison between these materials. Due to the significantly high epithermal flux for H_2O, we considered it as the best cooling liquid.

Table 2. Comparison of some in-air parameters for substrate materials.

backing plate material	N/(n/s)	$\Phi_{\rm epi}$/ (n/cm^{2}s)	$\dot{D}_{\gamma}/\Phi_{\rm epi}$/ (Gycm^2)
Al	8.63×10^{12}	1.61×10^{10}	1.60×10^{-13}
Cu	7.59×10^{12}	1.59×10^{10}	1.68×10^{-12}
W	7.11×10^{12}	1.21×10^{10}	3.74×10^{-12}
Ag	7.29×10^{12}	1.12×10^{10}	1.29×10^{-11}
Au	6.97×10^{12}	1.08×10^{10}	5.82×10^{-12}

Table 3. Comparison of epithermal neutron flux for the heat carrier.

cooling liquid	$\Phi_{\rm epi}$/(n/cm^{2}s)
H_2O	1.61×10^{10}
Hg	4.08×10^{8}
Ga	3.37×10^{8}

3.2.1 Target temperature

The values of parameters for calculating the lithium temperature are as follows. q=159.23W/cm^2 which is the heat flux deposited on the lithium target by a 2.5 MeV proton beam having 20 cm in diameter. Other parameters of the designed cooling system are: $\lambda_{\rm Li}$=84.7 W/m°K, $L=233.3$ μm (based on the result of the SRIM code for 2.5 MeV protons), $h_{\rm b}=0.5$ cm, $\lambda_{\rm b}$=250 W/m°K, λ=0.657 W/m°K, $d=1.2$ cm, $v=10$ m/s, $C_{\rm p}$=4.19 j/g°K, ν=1.004×10^{-6} m^2/s, ρ=1 g/cm^3 and $\alpha=3.04\times10^4$ W/m$^{2\circ}$K. According to these values, $\Delta T_{\rm Li}=0.4$ ℃, $\Delta T_{\rm b}=31$ ℃ and $\Delta T_{\rm b-h}=52$ ℃. Considering $T_0=20$ ℃, $T_{\rm Li}$ is 103.4 ℃ which is lower than the melting point of ^{7}Li. However, the practical diameter of the proton beam is in the range of centimeters. For a proton beam with 1 cm in diameter, the calculated heat flux deposited on the surface of the target is q=63694.27 W/cm^2. This high heat flux results in the melting of the lithium target. In order to avoid this problem, a new approach is proposed: utilizing the spot scanning irradiation based on the movement of beam area on the surface of the target. We propose to irradiate the area of the target for 4 ms and move the spot beam to another point. Considering this irradiation method for a uniform

distribution of the beam density, the temperature of the irradiated spot of the target reaches up to 154.7 ℃, and then it decreases until the spot beam returns to this position. Clearly, the proposed spot scanning in which the radius of the proton beam and lithium target are 0.5 and 10 cm, and the scanning frequency is over 16 Hz (the cycle period is less than 63 ms), prevents the melting of the target.

3.3 BSA optimization

3.3.1 Moderator

Figure 2 shows the calculated epithermal neutron flux corresponding to some materials as moderators versus their thicknesses.

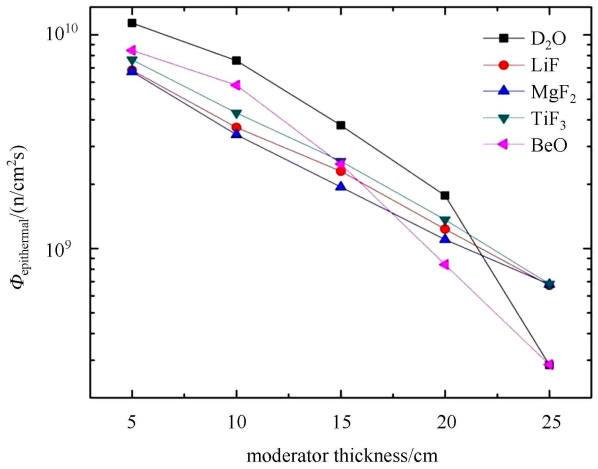

Fig. 2. (color online) Epithermal neutron flux for different thicknesses of suggested materials as moderators.

As one of the recommended IAEA parameters, the ratio of fast neutron dose rate to the epithermal neutron flux for different thicknesses of suggested materials was tested. The simulation results are shown in Fig. 3. Considering Figs. 2 and 3, 20 cm D_2O was selected as the moderator since its results satisfies both the high epithermal flux and low fast neutron dose to the epithermal neutron flux.

3.3.2 Reflector

The calculated in-air parameters for 5 proposed materials including different reflector radii are reported in Table 4. As it is seen, graphite is an appropriate

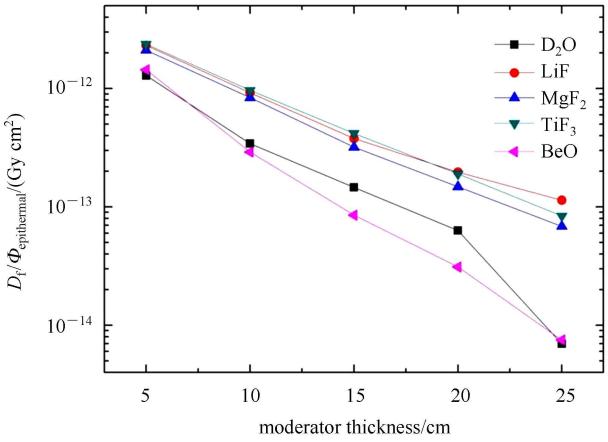

Fig. 3. (color online) Dose rate of fast neutron to epithermal flux for different thicknesses of moderators.

Table 4. The BNCT in-air parameters for different materials suggested as the reflector.

reflector material	radius/cm	$\Phi_{epithermal}$ ($\times10^9$ n/cm^{2}s)	$\Phi_{epithermal}/\Phi_{thermal}$	$\dot{D}_f/\Phi_{epithermal}$ ($\times10^{-13}$Gycm^2)	$\dot{D}_\gamma/\Phi_{epithermal}$ ($\times10^{-13}$Gycm^2)
Pb	13	1.78	2.19	0.60	1.34
	15	2.15	1.83	0.53	1.50
	20	2.74	1.56	0.48	2.33
	25	3.00	1.44	0.50	2.24
graphite	13	1.93	2.00	0.56	1.19
	15	2.36	1.47	0.48	1.56
	20	2.80	0.93	0.41	2.31
	25	2.93	0.78	0.39	3.09
BeO	13	2.04	1.81	0.53	1.86
	15	2.52	1.19	0.44	2.22
	20	2.94	0.74	0.39	3.36
	25	2.99	1.61	0.38	5.00
Ni	13	2.36	1.64	0.46	2.01
	15	3.00	1.45	0.39	3.47
	20	3.37	1.38	0.37	4.25
	25	3.48	1.39	0.38	4.35
Al_2O_3	13	1.87	2.29	0.60	2.18
	15	2.28	1.96	0.52	3.13
	20	2.78	1.58	0.44	5.95
	25	3.01	1.44	0.41	8.99

reflector. Also, to maintain the high epithermal flux and low fast neutron contamination simultaneously, 20 cm graphithe was selected as the optimized radius.

3.3.3 Thermal neutron filter

The results corresponding to utilizing four filters with 1 mm in thickness are presented in Table 5. Due to the good performance of Cd, it was chosen as the thermal neutron absorber.

Table 5. The BNCT in-air parameters for 4 different materials suggested as thermal neutron filters.

filter	$\Phi_{\rm epi}$/ (n/cm^{2}s)	$\Phi_{\rm epi}$/ $\Phi_{\rm thermal}$	$\dot{D}_{\rm f}/\Phi_{\rm epi}$/ Gycm^2	$\dot{D}_{\gamma}/\Phi_{\rm epi}$/ Gycm^2
^{6}Li	1.97×10^9	27.4	5.69×10^{-14}	3.30×10^{-13}
Li_2Co_3	1.59×10^9	93.2	6.80×10^{-14}	4.06×10^{-13}
Cd	2.63×10^9	110	4.21×10^{-14}	3.64×10^{-13}
^{10}B	7.64×10^8	70.2	1.36×10^{-13}	1.43×10^{-11}

3.3.4 Collimator

Table 6 shows the in-air parameters corresponding to BSAs with 6 different materials as the collimator. By the results, BeO was chosen as the most suitable collimator.

Table 6. BNCT in-air criteria at the end of BSA for 6 different materials as the collimator.

collimator	$\Phi_{\rm epi}$/ (n/cm^{2}s)	$\Phi_{\rm epi}$/ $\Phi_{\rm thermal}$	$\dot{D}_{\rm f}/\Phi_{\rm epi}$/ Gycm^2	$\dot{D}_{\gamma}/\Phi_{\rm epi}$/ Gycm^2
BeO	2.49×10^9	20.5	3.84×10^{-14}	2.23×10^{-13}
Li-Poly	1.81×10^9	105	3.97×10^{-14}	2.54×10^{-13}
Bi	2.11×10^9	12.5	3.83×10^{-14}	2.65×10^{-13}
Ni	2.75×10^9	55.9	3.07×10^{-14}	8.95×10^{-13}
Pb	2.24×10^9	16.9	3.79×10^{-14}	2.5×10^{-13}
Al_2O_3	2.26×10^9	20.8	3.92×10^{-14}	2.79×10^{-13}

The schematic designed BSA by using optimized materials is shown in Fig. 4. Table 7 presents the comparison between the in-air parameters related to this configuration and some published work. As can be seen, the proposed BSA based on the designed neutron source not only produces a higher epithermal neutron flux at the beam port, but also satisfies other IAEA criteria for BNCT of deep-seated tumors. Fig. 5 shows the neutron spectrum related to this configuration.

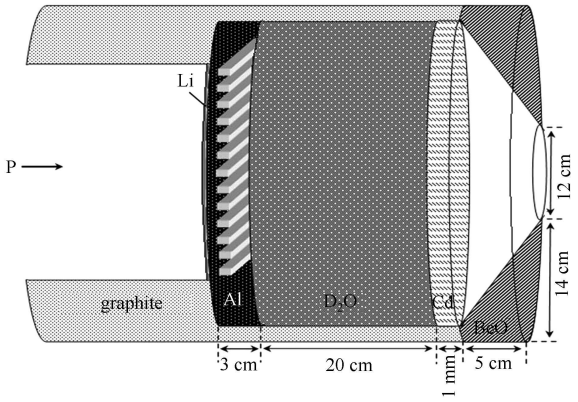

Fig. 4. A schematic view of the designed neutron source and the proposed BSA.

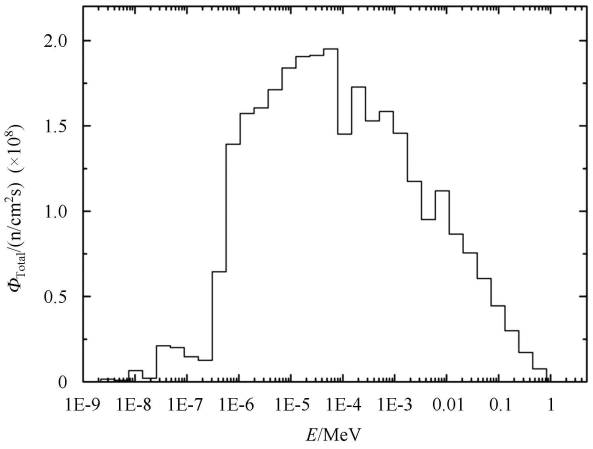

Fig. 5. (color online) Neutron spectrum related to the designed neutron source and the proposed BSA.

3.4 Dose evaluation

We consider the following values for dose calculation: $\omega_{\gamma}=1$, $\omega_{\rm N}=\omega_{\rm fast}=3.2$, and CBE is 1.3 in normal tissue and 3.8 in tumors. Boron concentration in normal tissue and tumors are 18 and 65 ppm, respectively.

Figure 6(a) shows the total delivered dose to the tumor and healthy tissue due to the irradiation of the designed beam to the simulated phantom. Also, the evaluated depth-dose profiles are shown in Fig. 6(b). Table 8 presents the in-phantom parameters corresponding to

Table 7. BNCT in-air parameters for the proposed BSA based on the designed neutron source and some published work.

references	facility	$\Phi_{\rm epithermal}$/ ($\times10^9$ n/cm^{2}s)	$\Phi_{\rm epithermal}$/ $\Phi_{\rm thermal}$	$\dot{D}_{\rm f}/\Phi_{\rm epithermal}$/ $\times10^{-13}$Gycm^2	$\dot{D}_{\gamma}/\Phi_{\rm epithermal}$/ $\times10^{-13}$Gycm^2
our work	^{7}Li(p,n)^{7}Be 2.5 MeV-20 mA	2.49	20.5	0.39	2.23
herrera et al. [16]	^{7}Li(p,n)^{7}Be 2.3 MeV-30 mA	0.95	125	5.2	4.9
Rahmani et al. [17]	photoneutron	0.819	3830	7.98	1.18
Montagini et al. [4]	D-T (2×10^{13}n/s)	0.29	16.6	6.3	7.3
Durisi et al. [18]	D-D	0.012	—	18.2	2.98

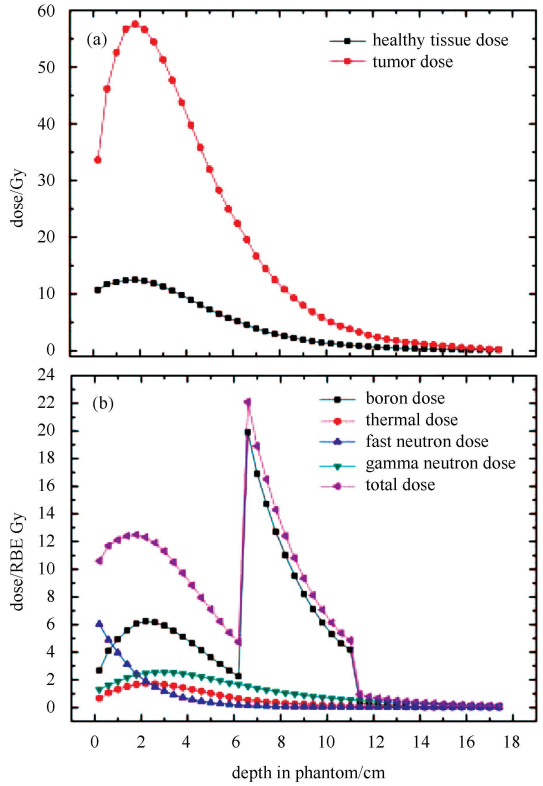

Fig. 6. (color online) (a): The evaluated depth-dose in the simulated head phantom with a centrally located tumor after 11.1 minutes irradiation of the designed beam. (b): The depth-dose profiles during treatment time.

Table 8. In-phantom parameters evaluated based on the designed neutron source.

ADDR/(Gy/min)	TT/min	AD/cm	AR
1.13	11.1	7.8	4.35

the irradiation of the designed beam. It can be seen that the designed BSA provides deep penetration of the therapeutic beam due to a relatively high AD value. Also, the reasonable treatment time, which is desired due to the practical considerations, makes the designed beam a suitable candidate for BNCT treatments.

4 Conclusion

A detailed study about an accelerator-based BNCT for a ^{7}Li(p,n)^{7}Be reaction with a 2.5 MeV-20 mA incident beam was carried out. Based on the MCNP simulation studies, it is found that lithium is the most suitable target material for this reaction due to its high neutron production compared with other lithium compositions. The target design was completed by using a cooling system which consists of Al as the backing plate and channels with H_2O flowing through them. In order to decrease the temperature of the target, the method of scanning irradiation of the proton beam was proposed. Calculations reveal that using this method, the target temperature reaches 154.7 ℃, which is lower than the melting point of lithium.

A beam shaping assembly was proposed based on the designed neutron source. The optimized configuration consists of D_2O as the moderator, Cd as the thermal neutron filter, graphite as the reflector, and BeO as the collimator. We show that the geometry and material of the reflector and collimator are important to have proper epithermal neutron flux. Our calculation show that the neutron beam related to the designed BSA not only contains a high epithermal flux (2.49×10^{9} n/cm^{2}s), but also the beam contamination is removed as much as possible and the IAEA recommended criteria are satisfied. A simulated Snyder head phantom consisting of skin, a skull, and a brain with a centrally located tumor was used for examination of the performance of the designed beam in tissue. The depth-dose curves and in-phantom parameters illustrate that the therapeutic beam related to the designed BSA is appropriate for BNCT of deep-seated brain tumors.

References

1 Bleuel D L, Donahue R J, Ludewigt B A, Vujic J. Med. Phys., 1998, **25**: 1725–1734
2 Sakamoto S, Kiger W S, Harling O K. Med. Phys., 1999, **26**: 1979–1998
3 Lee C L, ZHOU X L. Methods Phys. Res. B, 1999, **152**: 1–11
4 Montagnini B, Cerullo N, Esposito J, Giustia V et al. Phys. Res. A, 2002, **476**: 90–98
5 Blue T E, Yanch J C. J. Neuro-Onco., 2003, **62**: 19–31
6 Burlon A A, Kreiner A J. Nucl. Instrum. Methods Phys. Res. B, 2008, **266**: 763–771
7 Salehi D, Sardari D, Salehi Jozani M. Chinese Phys. C, 2013, **37**: 078201
8 CHENG D W, LU J B, YANG D et al. Chinese Phys. C, 2012, **36**: 905
9 IAEA-TECDOC-1223, 2001, International Atomic Energy Agency, 2001
10 Randers G, Brenner D J, Med. Phys., 1998, **25**: 894–896
11 Bayanov B, Belov V, Kindyuk V et al. Appl. Radiat. Isot., 2004, **61**: 817–821
12 KIM J K, KIM K O. Nucl. Eng. Technol., 2009, **41**: 531–544
13 Tanaka K, Yokobori H, Kobayashi E et al. Appl. Radiat. Isot., 2009, **67**: 259–265
14 Incropera F P, DeWitt P D. Introduction to Heat Transfer. 4th ed. Published: New York: Wiley, 2002
15 Rasouli F S, Masoudi S F, Kasesaz Y. Ann. Nucl. Energy., 2012, **39**: 18–25
16 Rahmani F, Shahriari M. Ann. Nucl. Energy, 2011, **38**: 404–409
17 Durisi E, Zanini A, Manfredotti C et al. Nucl. Instrum. Methods Phys. Res. A, 2007, **574**: 363–369
18 Herrera M S, Gonzalez S J, Minsky D M et al. Phys. Med., 2013, **29**: 436–449